Self-Consistent Theory of the Darrieus–Landau and Rayleigh–Taylor Instabilities with Self-Generated Magnetic Fields

F. García-Rubio,[1,2] R. Betti,[1,2,3] J. Sanz,[4] and H. Aluie[1,2]

[1]Laboratory for Laser Energetics, University of Rochester
[2]Department of Mechanical Engineering, University of Rochester
[3]Department of Physics and Astronomy, University of Rochester
[4]Escuela Técnica Superior de Ingeniería Aeronáutica y del Espacio, Universidad Politécnica de Madrid

The Rayleigh–Taylor instability (RT) has been thoroughly studied in the context of inertial confinement fusion (ICF).[1,2] In the weak acceleration regime, the cutoff wavelength is large compared to the ablation-front scale length, $k_{c0}L_a \ll 1$, and the dispersion relation can be analytically derived by exploiting the sharp-boundary model (SBM).[3,4] In the limit of zero acceleration, sufficiently long wavelengths undergo another type of instability known as Darrieus–Landau (DL). This instability is generic for fronts where a dense fluid expands into a lighter one, as typically occurs in flames.[5,6] During the development of these instabilities, magnetic (B) fields are generated due to the misalignment of gradients of density and pressure, known as baroclinic or the Biermann battery effect.[7] In the linear regime, the B field is coupled to the hydrodynamics mainly through the Righi–Leduc term. In essence, this term deflects the heat-flux lines, which in turn has a direct effect on the dynamics of these two instabilities.

In this summary, the Rayleigh–Taylor and Darrieus–Landau instabilities are studied in an ICF context within the framework of a small critical-to-shell density ratio D_R and a weak acceleration regime, i.e., large Froude number $Fr \gg 1$. This number stands for the ratio between ablative convection and the acceleration of the capsule. The two main novelties in this study are the inclusion of non-isobaric effects and the self-generated magnetic fields. The use of an SBM leads to a single analytical expression of the dispersion relation encompassing both instabilities:

$$\gamma = \frac{u_a}{L_a}\sqrt{\underbrace{\frac{kL_a}{Fr}}_{RT} - \underbrace{q_1(kL_a)^{8/5}}_{\text{perturbed pressure}} - \underbrace{\frac{1+f_1+q_2}{2}ku_a}_{\text{convective stabilization}}} \quad , \tag{1}$$

where u_a is the ablation velocity at the ablation front. The eigenvalues $\{f_i, q_i\}$ correspond to the perturbed mass and momentum fluxes through the ablation front, and $i = 1,2$ refers to its quasi-steady and nonstationary values, respectively. They depend only on the perturbation wavelength normalized with the conduction layer width, $kx_{c0} = 0.0117kL_a(2n_a/n_c)^{5/2}$, and are shown in Fig. 1.

For $kx_{c0} > 0.5$, the overpressure generated at the spikes q_1 is positive and becomes the main damping mechanism. For $kx_{c0} < 0.5$, q_1 is negative (underpressure) and destabilizing, becoming the driving mechanism of the DL instability. Asymptotic analysis allows one to derive the scaling laws of the underpressure for a small wave number. The non-isobaric effects play an important role for these perturbations, making q_1 scale as $q_1 = -5.8 (kx_{c0})^{11/15}$, compared to the isobaric case studied in Ref. 6, where $q_1 = -(5kx_{c0}/2)^{2/5}$.

Under the assumptions of the sharp boundary model, the effect of the self-generated magnetic field is always stabilizing. It increases both the momentum and mass fluxes. The Nernst convection enhances the stabilizing effect of the B field. For perturbation wavelengths longer than the distance between ablation front and critical surface, $kx_{c0} < 1$, the B field is less effective, becoming
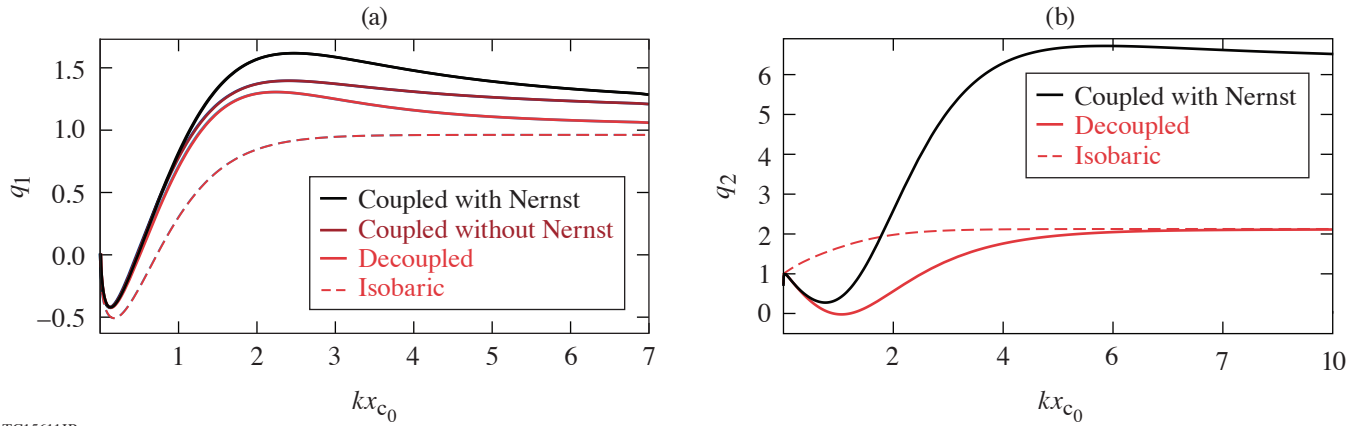
TC15611JR

Figure 1

Eigenvalues (a) q_1 and (b) q_2 (quasi-steady and nonsteady perturbed momentum flux). Black solid curve: coupled with Nernst; maroon solid curve: coupled without Nernst; red solid curve: B field decoupled; red dashed curve: results from the isobaric model in Ref. 6.

totally negligible in the DL instability region. The B-field effect is significantly stronger on the unsteady momentum flux q_2. This has an important effect on the convective stabilization term in Eq. (1), which is enhanced from "$-2ku_a$" to "$-4ku_a$."

The analysis of the dispersion relation reveals that the combination

$$D_R Fr^{2/3} = 0.015 \frac{\left(\dfrac{u_a}{1\,\mu m/ns}\right)^4 \left(\dfrac{n_a}{10^{24}\,cm^{-3}}\right)^{2/3}}{\left(\dfrac{g}{100\,\mu m/ns^2}\right)^{2/3} \left(\dfrac{T_a}{10\,eV}\right)^{8/3}} \tag{2}$$

dictates the behavior of the spectrum. For $D_R Fr^{2/3} \ll 1$, it is well described by the ablative RT instability in the isobaric regime, and the cutoff takes place for $kL_a \approx Fr^{-5/3}$. In the opposite limit, $D_R Fr^{2/3} \gg 1$, two regions can be defined. The long perturbations with $kL_a < D_R^{11/8}/Fr^{3/4}$ undergo RT instability, while the part of the spectrum with $kL_a < D_R^{11/8}/Fr^{3/4}$ is DL dominated. In this limit, the cutoff becomes independent of the Froude number: $kL_a \approx 7.6\,D_R^{5/2}$. The regime of application for ICF corresponds to $D_R Fr^{2/3} \lesssim 1$. When this parameter is close to unity, the DL effect operates by reducing the restoring overpressure and increasing the wave number at which ablation comes into play. It is precisely in this range, $D_R Fr^{2/3} \sim 1$, where the effect of the self-generated B fields becomes more important. They enhance the stabilizing effect of ablation and can significantly reduce the cutoff. A configuration of interest for ICF is shown in Fig. 2.
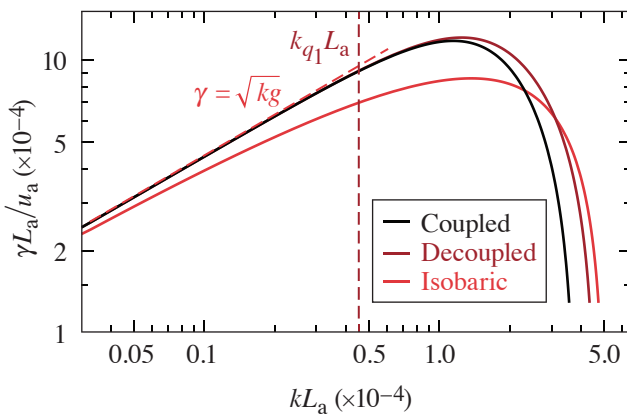
TC15612JR

Figure 2

Dispersion relation for $u_a = 1.2\,\mu m/ns$, $T_a = 7.5\,eV$, $n_a = 10^{24}\,cm^{-3}$, and $g = 50\,\mu m/ns^2$, which gives $Fr = 50$ and $D_R Fr^{2/3} = 0.11$. Black curve: magnetic fields and non-isobaric effects are included; maroon curve: non-isobaric effects are included, but the hydrodynamic is decoupled from induction; red curve: RT instability under the isobaricity assumption. The wave number where the perturbed pressure q_1 becomes positive is $k_{q_1}L_a = 4.4 \times 10^{-5}$.

A schematic of the different regimes supported in Eq. (1) is plotted in Fig. 3. In this schematic, the stability of a generic perturbation with wave number kL_a is given as a function of the Froude number and the critical- to shell-density ratio. It must be understood from an asymptotic analysis point of view; consequently, the transition from one region to another is blurry rather than a well-defined curve.
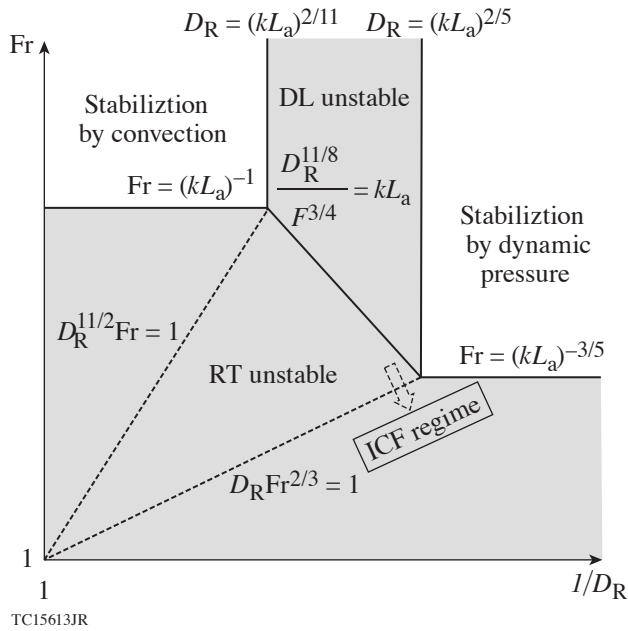
Figure 3

Schematic of the behavior of a given perturbation wave number kL_a as a function of the Froude number (Fr) and critical- to shell-density ratio D_R. The ICF regime corresponds to $D_R Fr^{2/3} \lesssim 1$.

1. H. J. Kull, Phys. Fluids B **1**, 170 (1989).

2. H. Takabe *et al.*, Phys. Fluids **28**, 3676 (1985).

3. J. Sanz, Phys. Rev. Lett. **73**, 2700 (1994).

4. V. N. Goncharov *et al.*, Phys. Plasmas **3**, 1402 (1996).

5. P. Clavin and L. Masse, Phys. Plasmas **11**, 690 (2004).

6. J. Sanz, L. Masse, and P. Clavin, Phys. Plasmas **13**, 102702 (2006).

7. K. Mima, T. Tajima, and J. N. Leboeuf, Phys. Rev. Lett. **41**, 1715 (1978).